the
abdus salam
international
centre
for theoretical
physics

united nations
educational, scientific
and cultural
organization

international atomic
energy agency

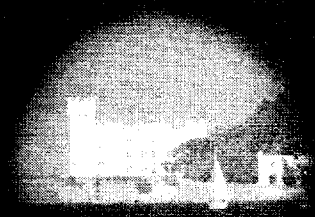

preprint

MULTI-DIMENSIONAL INSTABILITY OF ELECTROSTATIC SOLITARY STRUCTURES IN MAGNETIZED NONTHERMAL DUSTY PLASMAS

A.A. Mamun

S.M. Russel

César A. Mendoza-Briceño

M.N. Alam

T.K. Datta

and

A.K. Das

30 - 29

Available at: http://www.ictp.trieste.it/~pub_off IC/99/50

United Nations Educational Scientific and Cultural Organization
and
International Atomic Energy Agency
THE ABDUS SALAM INTERNATIONAL CENTRE FOR THEORETICAL PHYSICS

MULTI-DIMENSIONAL INSTABILITY OF ELECTROSTATIC SOLITARY STRUCTURES IN MAGNETIZED NONTHERMAL DUSTY PLASMAS

A.A. Mamun[1], S.M. Russel
Department of Physics, Jahangirnagar University, Savar, Dhaka, Bangladesh[2]
and
The Abdus Salam International Centre for Theoretical Physics, Trieste, Italy,

César A. Mendoza-Briceño
Centro de Astrofisica Teõrica, Universidad de los Andes, Merida, Venezuela[2]
and
The Abdus Salam International Centre for Theoretical Physics, Trieste, Italy

M.N. Alam, T.K. Datta[3] and A.K. Das[3]
Department of Physics, Jahangirnagar University, Savar, Dhaka, Bangladesh.

Abstract

A rigorous theoretical investigation has been made of multi-dimensional instability of obliquely propagating electrostatic solitary structures in a hot magnetized nonthermal dusty plasma which consists of a negatively charged hot dust fluid, Boltzmann distributed electrons, and nonthermally distributed ions. The Zakharov-Kuznetsov equation for the electrostatic solitary structures that exist in such a dusty plasma system is derived by the reductive perturbation method. The multi-dimensional instability of these solitary waves is also studied by the small-k (long wavelength plane wave) perturbation expansion method. The nature of these solitary structures, the instability criterion, and their growth rate depending on dust-temperature, external magnetic field, and obliqueness are discussed. The implications of these results to some space and astrophysical dusty plasma situations are briefly mentioned.

MIRAMARE – TRIESTE

May 1999

[1]Regular Associate of the Abdus Salam ICTP.
[2]Permanent address.
[3]INST, Atomic Energy Research Establishment, GPO Box 3787, Dhaka, Bangladesh.

1. Introduction

Recently, there has been a great deal of interest in understanding different types of collective processes in dusty plasmas (plasmas with extremely massive and negatively charged dust grains), because of its vital role in the study of astrophysical and space environments, such as, cometary tails, asteroid zones, planetary rings, interstellar medium, earth's environment, etc. [1-7]. These dust grains are negatively charged because of a number of charging processes, such as, field emission, ultra-violet radiation, plasma currents, etc. [8-10].

It has been found that the presence of static charged dust grains modifies the existing plasma wave spectra [11-18]. Bliokh and Yaroshenko [11] studied electrostatic waves in dusty plasmas and applied their results in interpreting spoke-like structures in Saturn's rings (revealed by Voyager space mission [19]). Angelis *et al.* [12] investigated the propagation of ion acoustic waves in a dusty plasma, in which a spatial inhomogeneity is created by a distribution of immobile dust particles [20]. They [12] applied their results in interpreting the low frequency noise enhancement observed by the *Vega and Giotto* space probes in the dusty regions of Halley's comet [21].

On the other hand, it has been shown both theoretically and experimentally that the dust charge dynamics introduces new eigenmodes, such as, dust-acoustic mode [22-26], dust ion-acoustic mode [27], dust cyclotron mode [28], dust drift mode [29-31], etc. Rao *et al.* [22] have first reported theoretically the existence of extremely low phase velocity (in comparison with the electron and ion thermal velocities) dust-acoustic waves in an unmagnetized dusty plasma whose constituents are an inertial charged dust fluid and Boltzmann distributed ions and electrons. Thus, in the dust-acoustic waves the dust particle mass provides the inertia and the pressures of electrons and ions give rise to the restoring force. This theoretical prediction of Rao *et al.* [22] has then been conclusively verified by laboratory experiments [25,26].

Recently, motivated by these theoretical and experimental studies [22,25,26], we have investigated dust-acoustic solitary structures in an unmagnetized dusty plasma system consisting of a negatively charged dust fluid and isothermal [32] or non-isothermal [33] ions. The present investigation has attempted to extend the earlier works [22,32,33] to the multi-dimensional instability of these electrostatic solitary structures propagating obliquely in a magnetized three-component dusty plasma. This dusty plasma system is assumed to consist of a negatively charged hot dust fluid, Boltzmann distributed electrons, and nonthermally distributed ions which have been found to exhibit by the numerical simulation studies on linear and nonlinear properties of dust-acoustic waves [34].

The manuscript is organized as follows. The governing equations are presented in section 2. The Zakharov-Kuznetsov (ZK) equation is derived by employing the reductive perturbation method in section 3. The solitary wave solution of this ZK equation is obtained and the properties of these electrostatic solitary structures are discussed in section 4. The instability criterion and the growth rate of these solitary structures are investigated in section 5. Finally, a brief discussion is presented in section 6.

2. Governing equations

We consider a three-component dusty plasma system consisting of extremely massive, micron-sized, negatively charged hot dust fluid, Boltzmann distributed electrons, and ions with fast

particles in the presence of an external static magnetic field ($\mathbf{B}_0 \parallel \hat{\mathbf{z}}$, where $\hat{\mathbf{z}}$ is a unit vector along the z-direction). Thus, at equilibrium we have $n_{i0} = Z_d n_0 + n_{e0}$, where n_{i0}, n_0, and n_{e0} are the unperturbed ion, dust, and electron number densities, respectively, and Z_d is the number of electrons residing on the dust grains. The dynamics of low phase velocity (lying between the ion and dust thermal velocities, viz., $v_{td} << v_p << v_{ti}$) dust-acoustic oscillations in such a magnetized dusty plasma is governed by [22,24,33]

$$\frac{\partial n}{\partial t} + \nabla \cdot (n\mathbf{u}) = 0, \tag{1}$$

$$\frac{\partial \mathbf{u}}{\partial t} + (\mathbf{u} \cdot \nabla)\mathbf{u} = \nabla\varphi - \omega_{cd}(\mathbf{u} \times \hat{\mathbf{z}}) - \frac{5}{3}\frac{\sigma_d}{n^{1/3}}\nabla n, \tag{2}$$

$$\nabla^2\varphi = n + (\frac{\mu}{1-\mu})e^{\sigma_i\varphi} - (\frac{1}{1-\mu})n_i, \tag{3}$$

where n is the the dust particle number density normalized to n_0; $\mathbf{u}$ is the dust fluid velocity normalized to the dust-acoustic speed $C_d = (Z_d T_i/m_d)^{1/2}$ with T_i being the ion-temperature (in energy units) and m_d being the mass of negatively charged dust particulates; $\sigma_d = T_d/Z_d T_i$ with T_d being the dust-temperature (in energy units); φ is the electrostatic wave potential normalized to T_i/e with e being the magnitude of the electron charge; $\sigma_i = T_i/T_e$; $\mu = n_{e0}/n_{i0}$; n_i is the ion number density normalized to n_{i0}. The time and space variables are in the units of the dust plasma period $\omega_{pd}^{-1} = (m_d/4\pi n_{d0} Z_d^2 e^2)^{1/2}$ and the Debye length $\lambda_{Dd} = (T_i/4\pi Z_d n_{d0} e^2)^{1/2}$, respectively. $\omega_{cd} = (Z_d e B_0/m_d)/\omega_{pd}$ is the dust cyclotron frequency normalized to ω_{pd}.

To model an ion distribution with a population of fast particles we can choose the distribution function as was chosen by Cairns *et. al* [35]. Therefore, the ion density n_i in (3) is directly given by

$$n_i = [1 + \frac{4\alpha}{1+3\alpha}(\varphi + \varphi^2)]e^{-\varphi}, \tag{4}$$

where α is a parameter determining the number of fast (nonthermal) ions [35,36]. It should be noted here that if we neglect the number of nonthermal ions in comparision with that of thermal ions, i.e. we put $\alpha = 0$, this dusty plasma model reduces to the model considered by Rao *et al.* [22].

3. Derivation of the ZK equation

We now follow the reductive perturbation technique and construct a weakly nonlinear theory for electrostatic waves with small but finite amplitude, which leads to a scaling of the independent variables through the stretched coordinates [37,38]

$$\left.\begin{array}{ll} x' = \epsilon^{1/2}x, & y' = \epsilon^{1/2}y, \\ z' = \epsilon^{1/2}(z - v_0 t), & t' = \epsilon^{3/2}t, \end{array}\right\} \tag{5}$$

where ϵ is a small parameter measuring the weakness of the dispersion and v_0 is the wave phase velocity. It may be noted here that x', y', z' are all normalized to the Debye length (λ_{Dd}), t' is normalized to the dust plasma period ($\omega_{pd}{}^{-1}$) and v_0 is normalized to the dust-acoustic speed (C_d). We can now expand the perturbed quantities about their equilibrium values in powers of ϵ as [37,38]

$$n = 1 + \epsilon n^{(1)} + \epsilon^2 n^{(2)} + \epsilon^3 n^{(3)} + \cdots,$$

$$
\begin{aligned}
\varphi &= 0 + \epsilon\varphi^{(1)} + \epsilon^2\varphi^{(2)} + \epsilon^3\varphi^{(3)} + \cdots, \\
u_z &= 0 + \epsilon u_z^{(1)} + \epsilon^2 u_z^{(2)} + \epsilon^3 u_z^{(3)} + \cdots, \\
u_x &= 0 + \epsilon^{3/2} u_x^{(1)} + \epsilon^2 u_x^{(2)} + \epsilon^{5/2} u_x^{(3)} + \cdots, \\
u_y &= 0 + \epsilon^{3/2} u_y^{(1)} + \epsilon^2 u_y^{(2)} + \epsilon^{5/2} u_y^{(3)} + \cdots.
\end{aligned} \tag{6}
$$

We now substitute (4) - (6) into (1) - (3) and develop equations in various powers of ϵ. To lowest order in ϵ, i.e., equating the coefficient of ϵ one can obtain the first order continuity equation, x-, y-, and z-components of the momentum equation, and Poisson's equation which in turn give

$$
\left.
\begin{aligned}
n^{(1)} &= \tfrac{1}{v_0} u_z^{(1)} = -\tfrac{1}{v_0^2 - \frac{5}{3}\sigma_d}\varphi^{(1)}, \\
n^{(1)} &= -[\tfrac{\sigma_i\mu}{1-\mu} + \tfrac{1}{1-\mu}(\tfrac{1-\alpha}{1+3\alpha})]\varphi^{(1)}, \\
u_x^{(1)} &= -\tfrac{1}{\omega_{cd}}[1 + \tfrac{5}{3}\sigma_d\{\tfrac{\sigma_i\mu}{1-\mu} + \tfrac{1}{1-\mu}(\tfrac{1-\alpha}{1+3\alpha})\}]\tfrac{\partial\varphi^{(1)}}{\partial y'}, \\
u_y^{(1)} &= \tfrac{1}{\omega_{cd}}[1 + \tfrac{5}{3}\sigma_d\{\tfrac{\sigma_i\mu}{1-\mu} + \tfrac{1}{1-\mu}(\tfrac{1-\alpha}{1+3\alpha})\}]\tfrac{\partial\varphi^{(1)}}{\partial x'}.
\end{aligned}
\right\} \tag{7}
$$

Here, the first two equations, give the linear dispersion relation

$$
v_0 = \sqrt{\frac{1}{\frac{1-\mu}{\sigma_i\mu + (1-\alpha)/(1+3\alpha)}} + \frac{5}{3}\sigma_d}, \tag{8}
$$

and the last two, respectively, represent the x- and y- components of $(\mathbf{V}_E + \mathbf{V}_D)$, where $\mathbf{V}_E$ and $\mathbf{V}_D$ are $\mathbf{E} \times \mathbf{B}_0$ and diamagnetic drifts, respectively. These last two equations are also satisfied by the next higher (second) order continuity equation. Similarly, to the next higher order of ϵ, we obtain the second order x- and y- components of the momentum equation and Poisson's equation as

$$
\left.
\begin{aligned}
u_x^{(2)} &= -\tfrac{v_0}{\omega_{cd}^2}[1 + \tfrac{5}{3}\sigma_d\{\tfrac{\sigma_i\mu}{1-\mu} + \tfrac{1}{1-\mu}(\tfrac{1-\alpha}{1+3\alpha})\}]\tfrac{\partial^2\varphi^{(1)}}{\partial z'\partial x'}, \\
u_y^{(2)} &= -\tfrac{v_0}{\omega_{cd}^2}[1 + \tfrac{5}{3}\sigma_d\{\tfrac{\sigma_i\mu}{1-\mu} + \tfrac{1}{1-\mu}(\tfrac{1-\alpha}{1+3\alpha})\}]\tfrac{\partial^2\varphi^{(1)}}{\partial z'\partial y'}, \\
(\tfrac{\partial^2}{\partial x'^2} + \tfrac{\partial^2}{\partial y'^2} + \tfrac{\partial^2}{\partial z'^2})\varphi^{(1)} &= n^{(2)} + [\tfrac{\sigma_i\mu}{1-\mu} + \tfrac{1}{1-\mu}(\tfrac{1-\alpha}{1+3\alpha})]\varphi^{(2)} - \tfrac{1}{2}(\tfrac{1-\sigma_i^2\mu}{1-\mu})[\varphi^{(1)}]^2.
\end{aligned}
\right\} \tag{9}
$$

The first two, respectively, denote the x- and y- components of dust polarisation drifts. Again, following the same procedure one can obtain the next higher order continuity equation and z-component of the momentum equation as

$$
\left.
\begin{aligned}
&\tfrac{\partial n^{(1)}}{\partial t'} - v_0\tfrac{\partial n^{(2)}}{\partial z'} + \tfrac{\partial u_x^{(2)}}{\partial x'} + \tfrac{\partial u_y^{(2)}}{\partial y'} + \tfrac{\partial}{\partial z'}[u_z^{(2)} + n^{(1)}u_z^{(1)}] = 0, \\
&\tfrac{\partial u_z^{(1)}}{\partial t'} - v_0\tfrac{\partial u_z^{(2)}}{\partial z'} + u_z^{(1)}\tfrac{\partial u_z^{(1)}}{\partial z'} - \tfrac{\partial\varphi^{(2)}}{\partial z'} + \tfrac{5}{3}\sigma_d\tfrac{\partial n^{(2)}}{\partial z'} = 0.
\end{aligned}
\right\} \tag{10}
$$

Now, using (7) - (10) we can readily obtain

$$
\frac{\partial\varphi^{(1)}}{\partial t'} + AB\varphi^{(1)}\frac{\partial\varphi^{(1)}}{\partial z'} + \frac{1}{2}A\frac{\partial}{\partial z'}[\frac{\partial^2}{\partial z'^2} + D(\frac{\partial^2}{\partial x'^2} + \frac{\partial^2}{\partial y'^2})]\varphi^{(1)} = 0, \tag{11}
$$

where

$$
\begin{aligned}
A &= [\frac{\sigma_i\mu}{1-\mu} + \frac{1}{1-\mu}\frac{1-\alpha}{1+3\alpha}]^{-3/2}[1 + \frac{5}{3}\sigma_d(\frac{\sigma_i\mu}{1-\mu} + \frac{1}{1-\mu}\frac{1-\alpha}{1+3\alpha})]^{-1/2}, \\
B &= \frac{1-\sigma_i^2\mu}{1-\mu} - 3[\frac{\sigma_i\mu}{1-\mu} + \frac{1}{1-\mu}\frac{1-\alpha}{1+3\alpha}]^2[1 + \frac{5}{3}\sigma_d(\frac{\sigma_i\mu}{1-\mu} + \frac{1}{1-\mu}\frac{1-\alpha}{1+3\alpha})], \\
D &= 1 + \frac{1}{\omega_{cd}^2}[1 + \frac{5}{3}\sigma_d(\frac{\sigma_i\mu}{1-\mu} + \frac{1}{1-\mu}\frac{1-\alpha}{1+3\alpha})]^2.
\end{aligned} \tag{12}
$$

This equation (11) is known as Zakharov-Kuznetsov (ZK) equation or Korteweg-de Vries (KdV) equation in three dimensions.

4. Solitary wave solution of the ZK equation

To study the solitary waves propagating in a direction making an angle δ with z'-axis, i.e., with the external magnetic field and lying in the (z'-x') plane we first rotate the co-ordinate axes (x', z') through an angle δ, keeping y'-axis fixed. Thus, we transform our independent variables to

$$\left.\begin{array}{ll} \zeta = x'\cos\delta - z'\sin\delta, & \eta = y', \\ \xi = x'\sin\delta + z'\cos\delta, & \tau = t.' \end{array}\right\} \tag{13}$$

This transformation of these independent variables makes us to write the ZK equation in the form

$$\begin{aligned} &\frac{\partial\varphi^{(1)}}{\partial\tau} + \delta_1\varphi^{(1)}\frac{\partial\varphi^{(1)}}{\partial\xi} + \delta_2\frac{\partial^3\varphi^{(1)}}{\partial\xi^3} + \delta_3\varphi^{(1)}\frac{\partial\varphi^{(1)}}{\partial\zeta} + \delta_4\frac{\partial^3\varphi^{(1)}}{\partial\zeta^3} \\ &\quad + \delta_5\frac{\partial^3\varphi^{(1)}}{\partial\xi^2\partial\zeta} + \delta_6\frac{\partial^3\varphi^{(1)}}{\partial\xi\partial\zeta^2} + \delta_7\frac{\partial^3\varphi^{(1)}}{\partial\xi\partial\eta^2} + \delta_8\frac{\partial^3\varphi^{(1)}}{\partial\zeta\partial\eta^2} = 0, \end{aligned} \tag{14}$$

where

$$\begin{aligned} \delta_1 &= AB\cos\delta, \\ \delta_2 &= \frac{1}{2}A(\cos^3\delta + D\sin^2\delta\cos\delta), \\ \delta_3 &= -AB\sin\delta, \\ \delta_4 &= -\frac{1}{2}A(\sin^3\delta + D\cos^2\delta\sin\delta), \\ \delta_5 &= A[D(\sin\delta\cos^2\delta - \frac{1}{2}\sin^3\delta) - \frac{3}{2}\cos^2\delta\sin\delta], \\ \delta_6 &= -A[D(\sin^2\delta\cos\delta - \frac{1}{2}\cos^3\delta) - \frac{3}{2}\cos\delta\sin^2\delta], \\ \delta_7 &= \frac{1}{2}AD\cos\delta, \\ \delta_8 &= -\frac{1}{2}AD\sin\delta. \end{aligned} \tag{15}$$

We now look for the steady state solution of this ZK equation in the form

$$\varphi^{(1)} = \varphi_0(Z),$$

where

$$Z = \xi - u_0\tau, \tag{16}$$

in which u_0 is a constant velocity normalized to the dust-acoustic speed (C_d). Using this transformation we can write this ZK equation in steady state form as

$$-u_0\frac{d\varphi_0}{dZ} + \delta_1\varphi_0\frac{d\varphi_0}{dZ} + \delta_2\frac{d^3\varphi_0}{dZ^3} = 0. \tag{17}$$

Now, using the appropriate boundary conditions, viz., $\varphi_0 \to 0$, $\frac{d\varphi_0}{dZ} \to 0$, $\frac{d^2\varphi_0}{dZ2} \to 0$ at $Z \to \pm\infty$, the solution of this equation is given by

$$\varphi_0(Z) = \varphi_{0m}\mathrm{sech}^2(Z/\Delta), \tag{18}$$

where $\varphi_{0m} = 3u_0/\delta_1$ is the height and $\Delta = \sqrt{4\delta_2/u_0}$ is the width (normalized to the λ_{Dd}) of the solitary potential. It is clear from (12) and (15) that as μ and α are always less than 1, i.e., $A > 0$, depending on whether B is positive or negative the solitary waves will be either compressive ($\varphi_{0m} < 0$) or rarefactive ($\varphi_{0m} > 0$). Therefore, for $\sigma_d = 0$ there exist solitary waves with negative potential (which are compressive solitary waves) when $B < 0$, i.e., $\alpha < (\sqrt{3}-1)/(\sqrt{3}+3) \simeq 0.155$ and solitary waves with positive potential (which are rarefactive solitary waves) when $B > 0$. It is clear that for $\sigma_d = 0$ there exist rarefactive solitary waves when $\alpha > (\sqrt{3}-1)/(\sqrt{3}+3) \simeq 0.155$. As we increase the dust fluid temperature, the minimum value of α, for which rarefactive dust-acoustic solitary structures exist, increases. Figure 1 shows how this minimum value of α increases with the dust fluid temperature. It is also shown from (12), (15), and (18) that the height of both the compressive and rarefactive solitary waves is a nonlinear function of obliqueness δ and dust fluid temperature σ_d. Figure 2 shows how the height of both the compressive and rarefactive solitary waves increases with the obliqueness δ and with the dust fluid temperature σ_d. The magnitude of the external magnetic field has no any direct effect on the amplitude of these solitary waves. However, it does have a direct effect on the width of these solitary waves. Figures 3 and 4 show how the width Δ of these solitary waves changes with σ_d, δ, and ω_{cd}. These show that the width of both the compressive and rarefactive solitary waves increases with both δ and σ_d but decreases with the external magnetic field.

It is obvious from (15) and (18) that for large angles ($\delta \sim 90°$) the width goes to 0 and amplitude goes to ∞. It is likely that for large angles the assumption that the waves are electrostatic is no longer valid one, and we should look for fully electromagnetic structures.

5. Instability analysis

We now study the instability of the obliquely propagating solitary waves, discussed in the previous section, by the method of small-k perturbation expansion method [39-41]. We first assume that

$$\varphi^{(1)} = \varphi_0(Z) + \varphi(Z, \zeta, \eta, \tau), \tag{19}$$

where φ_0 is defined by (18) and φ, for a long-wavelength plane wave perturbation in a direction with cosines (l_ζ, l_η, l_ξ), is given by

$$\varphi = \psi(Z) e^{i[k(l_\zeta \zeta + l_\eta \eta + l_\xi Z) - \omega\tau]}, \tag{20}$$

in which $l_\zeta^2 + l_\eta^2 + l_\xi^2 = 1$ and, $\psi(Z)$ and ω, for small k, can be expanded as [39-41]

$$\left.\begin{aligned} \psi(Z) &= \psi_0(Z) + k\psi_1(Z) + k^2\psi_2(Z) + \cdots, \\ \omega &= 0 + k\omega_1 + k^2\omega_2 + \cdots. \end{aligned}\right\} \tag{21}$$

Now, substituting (21) into (14) and linearizing with respect to φ, we can express the linearized ZK equation in the form

$$\begin{aligned} \frac{\partial\varphi}{\partial\tau} - u_0\frac{\partial\varphi}{\partial Z} + \delta_1\varphi_0\frac{\partial\varphi}{\partial Z} + \delta_1\varphi\frac{\partial\varphi_0}{\partial Z} + \delta_2\frac{\partial^3\varphi}{\partial Z^3} + \delta_3\varphi_0\frac{\partial\varphi}{\partial\zeta} + \delta_4\frac{\partial^3\varphi}{\partial\zeta^3} \\ + \delta_5\frac{\partial^3\varphi}{\partial Z^2\partial\zeta} + \delta_6\frac{\partial^3\varphi}{\partial Z\partial\zeta^2} + \delta_7\frac{\partial^3\varphi}{\partial Z\partial\eta^2} + \delta_8\frac{\partial^3\varphi}{\partial\zeta\partial\eta^2} = 0. \end{aligned} \tag{22}$$

Our main object is now to find ω_1 by solving zeroth-, first-, and second-order equations obtained from these last three equations. Using (20) - (22), the zeroth-order equation can be written, after integration, as

$$(-u_0 + \delta_1\varphi_0)\psi_0 + \delta_2\frac{d^2\psi_0}{dZ^2} = C, \tag{23}$$

where C is an integration constant. It is clear from (17) that the homogeneous part of this equation has two linearly independent solutions, namely

$$f = \frac{d\varphi_0}{dZ}, \tag{24}$$

$$g = f\int^Z \frac{dZ}{f^2}. \tag{25}$$

Therefore, the general solution of this zeroth order equation can be written as

$$\psi_0 = C_1 f + C_2 g - Cf\int^Z \frac{g}{W}dZ + Cg\int^Z \frac{f}{W}dZ, \tag{26}$$

where C_1 and C_2 are two constants and W is the Wronskian defined by $W = f\frac{dg}{dZ} - g\frac{df}{dZ}$. Now, evaluating all integrals, the general solution of this zeroth-order equation, for ψ_0 not tending to $\pm\infty$ as $Z \to \pm\infty$, can finally be simplified to

$$\psi_0 = C_1 f. \tag{27}$$

The first-order equation, i.e., equation with terms linear in k, obtained from (20) - (22) and (27), can be expressed, after integration, as

$$(-u_0 + \delta_1\varphi_0)\psi_1 + \delta_2\frac{d^2\psi_1}{dZ^2} = iC_1[\alpha_1 + \beta_1\tan^2(Z/\Delta)]\varphi_0 + K, \tag{28}$$

where K is the integration constant and α_1 and β_1 are given by

$$\left.\begin{array}{l} \alpha_1 = (\omega_1 + l_\xi u_0) - \frac{1}{2}\varphi_{0m}\mu_1 + 2\mu_2/\Delta^2, \\ \beta_1 = \frac{1}{2}\varphi_{0m}\mu_1 - 6\mu_2/\Delta^2, \\ \mu_1 = \delta_1 l_\xi + \delta_3 l_\zeta, \\ \mu_2 = 3\delta_2 l_\xi + \delta_5 l_\zeta. \end{array}\right\} \tag{29}$$

Now, following the same procedure the general solution of this first-order equation, for ψ_1 not tending to $\pm\infty$ as $Z \to \pm\infty$, can be expressed as

$$\psi_1 = K_1 f + \frac{iC_1\Delta^2}{8\delta_2}[(\alpha_1 + \beta_1)Zf + \frac{2}{3}(3\alpha_1 + \beta_1)\varphi_0]. \tag{30}$$

The second-order equation, i.e., equation with terms involving k^2, obtained from (20)–(22), can be written as

$$[-u_0\frac{d}{dZ} + \delta_1\frac{d}{dZ}\varphi_0 + \delta_2\frac{d^3}{dZ^3}]\psi_2 = i\omega_2\psi_0 + i(\omega_1 + l_\xi u_0)\psi_1 - i\mu_1\varphi_0\psi_1 + \mu_3\frac{d\psi_0}{dZ} - i\mu_2\frac{d^2\psi_1}{dZ^2}, \tag{31}$$

where

$$\mu_3 = 3\delta_2 l_\xi^2 + 2\delta_5 l_\zeta l_\xi + \delta_6 l_\zeta^2 + \delta_7 l_\eta^2. \tag{32}$$

The solution of this second-order equation exists, if the right-hand side is orthogonal to a kernel of the operator adjoint to the operator

$$-u_0\frac{d}{dZ}+\delta_1\frac{d}{dZ}\varphi_0+\delta_2\frac{d^3}{dZ^3}. \tag{33}$$

This kernel, which must tend to zero as $Z\to\pm\infty$, is $\varphi_0/\varphi_{0m}=\mathrm{sech}^2(Z/\Delta)$. Thus, we can write the following equation determining ω_1:

$$\int_{-\infty}^{\infty}\varphi_0[i\omega_2\psi_0+i(\omega_1+l_\xi u_0)\psi_1-i\mu_1\varphi_0\psi_1+\mu_3\frac{d\psi_0}{dZ}-i\mu_2\frac{d^2\psi_1}{dZ^2}]dZ=0. \tag{34}$$

Now, substituting the expressions for ψ_0 and ψ_1 given, respectively, by (27) and (30), and then performing the integration, we arrive at the dispersion relation:

$$\omega_1=\Omega-l_\xi u_0+\sqrt{\Omega^2-\Upsilon}, \tag{35}$$

where

$$\left.\begin{array}{l}\Omega=\frac{2}{3}(\varphi_{0m}\mu_1-2\mu_2/\Delta^2),\\ \Upsilon=\frac{16}{45}(\varphi_{0m}^2\mu_1^2-3\varphi_{0m}\mu_1\mu_2/\Delta^2-3\mu_2^2/\Delta^4+12\mu_3/\Delta^4).\end{array}\right\} \tag{36}$$

It is clear from our dispersion relation (35) that there is always instability if $\Upsilon-\Omega^2>0$. Thus, using (12), (15), (29), (32) and (36) we can express this instability criterion as

$$\left.\begin{array}{l}S_i>0,\\ S_i=[1+\frac{l_\zeta^2}{l_\eta^2}(1-\frac{5}{3}\tan^2\delta)]\omega_{cd}^2+(\sin^2\delta-\frac{l_\zeta^2}{l_\eta^2}\tan^2\delta)T_d^2,\\ T_d=1+\frac{5}{3}\sigma_d[\frac{\sigma_i\mu}{1-\mu}+\frac{1}{1-\mu}(\frac{1-\alpha}{1+3\alpha})].\end{array}\right\} \tag{37}$$

and the growth rate γ of this instability as

$$\gamma=\frac{2}{\sqrt{135}}\frac{u_0 l_\eta}{\omega_{cd}(\cos^2\delta+D\sin^2\delta)}\sqrt{DS_i} \tag{38}$$

where D is given in (12). It is clear that the growth rate (γ) is a nonlinear function of σ_d, α, and ω_{cd}. Figures 7 and 8 show how γ changes with these parameters. Now, differentiating S_i with respect to ω_{cd}^2 one can obtain

$$\begin{aligned}\frac{\partial S_i}{\partial\omega_{cd}^2} &= 1+\frac{l_\zeta^2}{l_\eta^2}(1-\frac{5}{3}\tan^2\delta)\\ &= [(1+\frac{8}{3}\frac{l_\zeta^2}{l_\eta^2})\cos^2\delta-\frac{5}{3}\frac{l_\zeta^2}{l_\eta^2}]\frac{1}{\cos^2\delta}.\end{aligned} \tag{39}$$

This means that if $(1+\frac{l_\eta^2}{l_\zeta^2})>(<)\frac{5}{3}\tan^2\delta$, S_i increases (decreases) with ω_{cd}^2. The condition $S_i=0$, which expresses the threshold value of ω_{cd} in terms of $\frac{l_\zeta}{l_\eta}$ and δ, can be written as

$$\omega_{cd}^2=\frac{(1-\cos^2\delta)(\frac{5}{3}\frac{l_\zeta^2}{l_\eta^2}-\cos^2\delta)}{(1+\frac{8}{3}\frac{l_\zeta^2}{l_\eta^2})\cos^2\delta-\frac{5}{3}\frac{l_\zeta^2}{l_\eta^2}}[1+\frac{5}{3}\sigma_d\{\frac{\sigma_i\mu}{1-\mu}+\frac{1}{1-\mu}(\frac{1-\alpha}{1+3\alpha})\}]. \tag{40}$$

Therefore, ω_{cd}^2 has a resonance at

$$\delta_\infty=\cos^{-1}[\sqrt{\frac{5}{3}\frac{l_\zeta^2}{l_\eta^2}/(1+\frac{8}{3}\frac{l_\zeta^2}{l_\eta^2})}] \tag{41}$$

and zero at

$$\delta_0 = 0 \quad \text{when} \quad \frac{l_\zeta}{l_\eta} > \sqrt{\frac{3}{5}},$$

$$\delta_0 = \cos^{-1}\sqrt{[\frac{5}{3}\frac{l_\zeta^2}{l_\eta^2}]} \quad \text{when} \quad \frac{l_\zeta}{l_\eta} < \sqrt{\frac{3}{5}}. \tag{42}$$

We note from (39)–(42) that for $\delta_0 < \delta < \delta_\infty$, $\frac{\partial S_i}{\partial \omega_{cd}^2} > 0$, i.e., the instability region lies above $S_i = 0$ for both $l_\zeta/l_\eta > \sqrt{3/5}$ and $l_\zeta/l_\eta < \sqrt{3/5}$. Thus, we have two cases, depending on whether $\frac{l_\zeta}{l_\eta}$ is larger or smaller than $\sqrt{3/5}$. Figures 5 and 6 show how the instability regions in these two cases depend on ω_{cd}, δ, and σ_d. It is shown that the minimum/maximum value of δ for which the waves become unstable, is independent of the dust fluid temperature.

6. Discussion

A three component magnetized dusty plasma system consisting of negatively charged hot dust fluid, Boltzmann distributed electrons, and nonthermally distributed ions has been considered and the properties of finite amplitude electrostatic solitary structures and their multidimensional instability have been investigated. We have derived the Zakharov Kuznetsov (ZK) equation by the reductive perturbation method and then analyzed the stability of these structures by small-k expansion method. The results, which have been found in this investigation, may be pointed out as follows:

i) The effects of nonthermal ions and dust fluid temperature have been found to modify the nature of the electrostatic solitary structures in a dusty plasma. It has been shown that the presence of nonthermal/fast ions may allow compressive and rarefactive solitary waves to exist. It is found that, depending on the value of α, the solitary structures may change from compressive to rarefactive and that for cold dust fluid there exist solitary waves with negative (positive) potential, i.e., compressive (rarefactive) solitary waves when $\alpha < (>)0.155$. It is shown that as we increase the dust fluid temperature, we need higher value of α in order to have rarefactive solitary waves (Figure 1). It is also shown that the height and width of these solitary structures increase with the dust fluid temperature (Figures 2 and 3).

ii) The effects of the obliqueness and the external magnetic field make these solitary structures unstable and change the height and width of these solitary structures. It is found that the height of both the compressive and rarefactive solitary waves is inversely proportional to $\cos\delta$ [Eqs. (15) and (18)]. It is shown that the width of these solitary waves increases with δ for its lower range (Figure 3). We already pointed out that for large angles the assumption that the waves are electrostatic is no longer a valid one, and we should look for fully electromagnetic structures. The magnitude of the external magnetic field $\mathbf{B}_0$ has no direct effect on the amplitude of these solitary waves. However, it does have a direct effect on their width. We have found that as its magnitude increases, the width of both the compressive and rarefactive solitary waves decreases, i.e., the external magnetic field makes the solitary structures more spiky (Figure 4).

iii) We have shown that the α-value has no effect on whether the solitary waves will be stable or unstable. However, stability of these solitary structures strongly depend on the external magnetic field and the propagation directions of both the nonlinear waves and their perturbation

mode. We have drawn plots of $S_i = 0$ (Figures 5 and 6) in parameter space (ω_{cd}, δ, σ_d) and shown two instability regions for two different cases, namely, $\frac{l_\zeta}{l_\eta} > \sqrt{\frac{3}{5}}$ and $\frac{l_\zeta}{l_\eta} < \sqrt{\frac{3}{5}}$. The dust fluid temperature has no effect on the minimum/maximum value of δ for which solitary waves are unstable [Eqs. (41) and (42)]. It is found that when $\frac{l_\zeta}{l_\eta} = 0.8$, the waves become unstable for $0° < \delta < 40°$ (Figure 5) and when $\frac{l_\zeta}{l_\eta} = 0.7$, the waves become unstable for $25° < \delta < 47°$ (Figure 6). It is shown that as we increase the dust-fluid temperature, the unstable region decreases for both $\frac{l_\zeta}{l_\eta} > \sqrt{\frac{3}{5}}$ (Figure 5) and $\frac{l_\zeta}{l_\eta} < \sqrt{\frac{3}{5}}$ (Figure 6).

iv) It is also shown that the growth rate (γ) of this instability increases with dust-fluid temperature but decreases with the number of nonthermal ions (α) (Figure 7). It is also found that the growth rate decreases with the external magnetic field (ω_{cd}) but increases with the obliqueness (δ) (Figure 8).

We have analyzed instability of these solitary structures by the reductive perturbation method and small-k perturbation expansion which are valid for small but finite amplitude solitary waves and long wavelength perturbation mode. Since in many astrophysical situations there may exist extremely large amplitude solitary waves and short wavelength perturbation mode, we propose to develop a more exact theory for stability analysis of arbitrary-amplitude solitary waves and arbitrary wavelength perturbation modes by generalization of our present work to such waves and modes. However, our present analysis should be useful for understanding different nonlinear features of localized and unstable electrostatic disturbances in a number of astrophysical dusty plasma systems, such as, planetary ring systems (viz. Saturn's rings [3,11,19]), cometary environment (viz. Halley's comet [12,21]), interstellar medium [3], etc., where negatively charged dust particulates and Boltzmann distributed electrons and thermally/nonthermally distributed ions are the major plasma species. This investigation should also be important in understanding coagolation or condensation of the dust grains in such space and astrophysical dusty plasma systems.

It may be added that the effects of dust grain charge fluctuation and inhomogeneity in plasma density and magnetic field on these electrostatic solitary structures are also problems of great importance but beyond the scope of the present work.

Acknowledgements

One of the authors (AAM) is grateful to Prof. P. K. Shukla, Prof. R. A. Cairns, Prof. M. A. Hassan, and Dr. Y. Hayashi for their invaluable suggestions and stimulating discussions during the course of this work. This work was done within the framework of the Associateship Scheme of the Abdus Salam International Centre for Theoretical Physics, Trieste, Italy. AAM and SMR would like to acknowledge the financial support of the Abdus Salam ICTP. Financial support from the Swedish International Development Cooperation Agency is also acknowledged.

References

[1] Horanyi, M. and Mendis, D. A., Astrophys. J. **294**, 357 (1985).

[2] Horanyi, M. and Mendis, D. A., Astrophys. J. **307**, 800 (1986).

[3] Goertz, C. K., Rev. Geophys. **27**, 271 (1989).

[4] Northrop, T. G., Phys. Scripta **45**, 475 (1992).

[5] Mendis, D. A. and Rosenbeg, M., IEEE Trans. Plasma Sci. **20**, 929 (1992).

[6] Mendis, D. A. and Rosenberg, M., Annu. Rev. Astron. Astrophys. **32**, 419 (1994).

[7] Verheest, F., Space Sci. Rev. **77**, 267 (1996).

[8] Feuerbacher, B., Willis, R. T. and Fitton, B., Astrophys. J. **181**, 101 (1973).

[9] Fechting, H., Grun, E. and Morfill, G. E., Planet. Space Sci. **27**, 511 (1979).

[10] Havnes, O., Goertz, C. K., Morfill, G. E. and Ip, W., J. Geophys. Res. **92**, 2281 (1987).

[11] Bliokh, P. V. and Yaroshenko, V. V., Sov. Astron. (Engl. Transl.) **29**, 330 (1985).

[12] Angelis, U. de, Formisano, V. and Giordano, M., J. Plasma Phys. **40**, 399 (1988).

[13] Angelis, U. de, Bingham, R. and Tsytovich, V. N., J. Plasma Phys. **42**, 445 (1989).

[14] D'Angelo, N., Planet. Space Sci. **38**, 9 (1990).

[15] Bingham, R., Angelis, U. de, Tsytovich, V. N. and Havnes, O., Phys. Fluids B **3**, 811 (1991).

[16] Shukla, P. K. and Stenflo, L., Astrophys. Space Sci. **190**, 23 (1992).

[17] Angelis, U. de, Forlani, A., Bingham, R., Shukla, P. K., Ponomarev, A. and Tsytovich, V. N., Phys. Plasmas 1, 236 (1994).

[18] Shukla, P. K. and Vladimirov, S. V., Phys. Plasmas **2**, 3179 (1995).

[19] Smith, B. A., *et al.*, A New Look at the Saturn System: The Voyager 2 Images, Science **215**, 504 (1982).

[20] Whipple, E. C., Northrop, T. G. and Mendis, D. A., J. Geophys. Res. **90**, 7405 (1985).

[21] Pedersen, A., Grard, R., Teotgnon, J. G., Beghin, C., Mihailov, M. and Mogilevsky, M., Proceedings of International Symposium on Exploration of Halley's Comet, Heidelberg, vol. 3 (ed. B. Battrick, E. J. Rolfe and R. Reinhard) p. 425, ESA Publications Division, ESA SP-250 (1987).

[22] Rao, N. N, Shukla, P. K. and Yu, M. Y., Planet. Space Sci. **38**, 543 (1990).

[23] Melandø, F., Aslaksen, T. K. and Havnes, O., Planet. Space Sci. **41**, 321 (1993).

[24] Rosenberg, M., Planet. Space Sci. **41**, 229 (1993).

[25] Barkan, A., Merlino, R. L. and D'Angelo, N., Phys. Plasmas **2**, 3563 (1995).

[26] D'Angelo, N., J. Phys. D **28**, 1009 (1995).

[27] Shukla, P. K. and Silin, V. P., Phys. Scripta **45**, 508 (1992).

[28] Shukla, P. K. and Rahman, H. U., Planet. Space Sci. **46**, 541 (1998).

[29] Shukla, P. K., Yu, M. Y. and Bharuthram, R., J. Geophys. Res. **96**, 21343 (1991).

[30] Mamun, A. A., Salahuddin, M. and Salimullah, M., Planet. Space Sci. **47**, 79 (1999).

[31] Salimullah, M., Salahuddin M. and Mamun, A. A., Astrophys. Space Sci. **260**, 000 (1999).

[32] Mamun, A. A., Cairns, R. A. and Shukla, P. K., Phys. Plasmas **3**, 702 (1996).

[33] Mamun, A. A., Cairns, R. A. and Shukla, P. K., Phys. Plasmas **3**, 2610 (1996).

[34] Winske, D., Gary, S. P, Jones, E., Rosenberg, M., Chow, V. W., and Mendis, D. A., Geophys. Res. Lett. **22**, 2069 (1995).

[35] Cairns, R. A., Mamun, A. A., Bingham, R., Dendy, R. O., Bostrom, R., Shukla, P. K., and Nairn, C. M. C., Geophys. Res. Lett. **22**, 2709 (1995).

[36] Mamun, A. A., Phys. Rev. E **55**, 1852 (1997).

[37] Laedke, E. W. and Spatschek, K. H., J. Plasma Phys. **28**, 469 (1982).

[38] Infeld, E., J. Plasma Phys. **33**, 171 (1985).

[39] Rowlands, G., J. Plasma Phys. **3**, 569 (1969).

[40] Infeld, E., J. Plasma Phys. **8**, 105 (1972).

[41] Infeld E., and Rowlands, G., J. Plasma Phys. **10**, 293 (1973).

FIGURE CAPTIONS

Figure 1: Variation of B with α for $\mu = 0.25$, $u_0 = 1.0$, $\sigma_i = 0.10$, $\sigma_d = 0.01$ (solid curve), $\sigma_d = 0.1$ (dashed curve), and $\sigma_d = 0.2$ (dotted curve).

Figure 2: Variation of the amplitude (ϕ_{0m}) with the dust fluid temperature σ_d for $\alpha = 0.2$, $u_0 = 1.0$, $\omega_{cd} = 0.1$, $\mu = 0.25$, $\sigma_i = 0.1$, $\delta = 5^\circ$ (solid curve), $\delta = 15^\circ$ (dashed curve), and $\delta = 30^\circ$ (dotted curve).

Figure 3: Variation of the width (Δ) with the dust fluid temperature σ_d for $\alpha = 0.2$, $u_0 = 1.0$, $\omega_{cd} = 0.1$, $\mu = 0.25$, $\sigma_i = 0.1$, $\delta = 5^\circ$ (solid curve), $\delta = 15^\circ$ (dashed curve), and $\delta = 30^\circ$ (dotted curve).

Figure 4: Variation of the width (Δ) with ω_{cd} for $\mu = 0.25$, $u_0 = 1.0$, $\sigma_i = 0.10$, $\sigma_d = 0.01$ (solid curve), $\sigma_d = 0.1$ (dashed curve), and $\sigma_d = 0.2$ (dotted curve).

Figure 5: Plot of $S_i = 0$ in parameter space (ω_{cd}, δ, σ_d) showing an instability region for $l_\zeta/l_\eta = 0.8$, $\sigma_d = 0.01$ (solid curve), $\sigma_d = 0.1$ (dashed curve), and $\sigma_d = 0.2$ (dotted curve).

Figure 6: Plot of $S_i = 0$ in parameter space (ω_{cd}, δ, σ_d) showing an instability region for $l_\zeta/l_\eta = 0.7$, $\sigma_d = 0.01$ (solid curve), $\sigma_d = 0.1$ (dashed curve), and $\sigma_d = 0.2$ (dotted curve).

Figure 7: Variation of the growth rate (γ) with σ_d for $\delta = 15^\circ$, $\omega_{cd} = 0.1$, $\mu = 0.25$, $u_0 = 1.0$, $\sigma_i = 0.10$, $l_\zeta/l_\eta = 0.8$, $\alpha = 0.2$ (solid curve), $\alpha = 0.3$ (dashed curve), and $\alpha = 0.4$ (dotted curve).

Figure 8: Variation of the growth rate (γ) with ω_{cd} for $\alpha = 0.2$, $\sigma_d = 0.1$, $\mu = 0.25$, $\sigma_i = 0.1$, $u_0 = 1.0$, $l_\zeta/l_\eta = 0.7$, $\delta = 5^\circ$ (solid curve), $\delta = 15^\circ$ (dashed curve), and $\delta = 30^\circ$ (dotted curve).

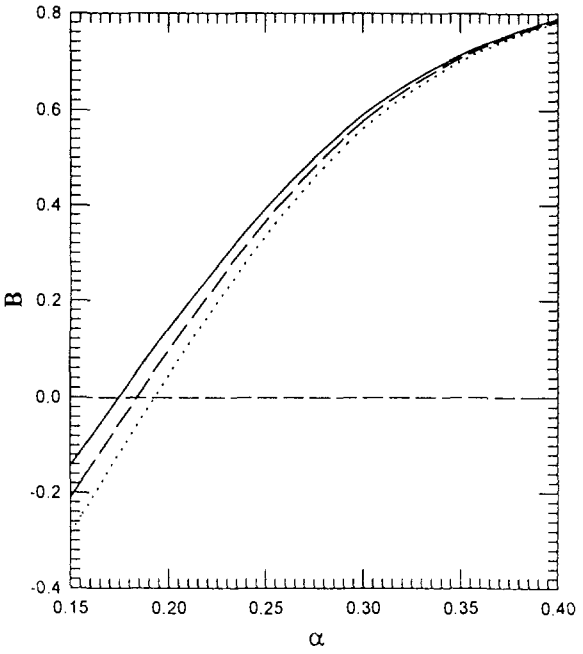
0.8
0.6
0.4
0.2
0.0
-0.2
-0.4
B
0.15
0.20
0.25
0.30
0.35
0.40
α

Fig.1

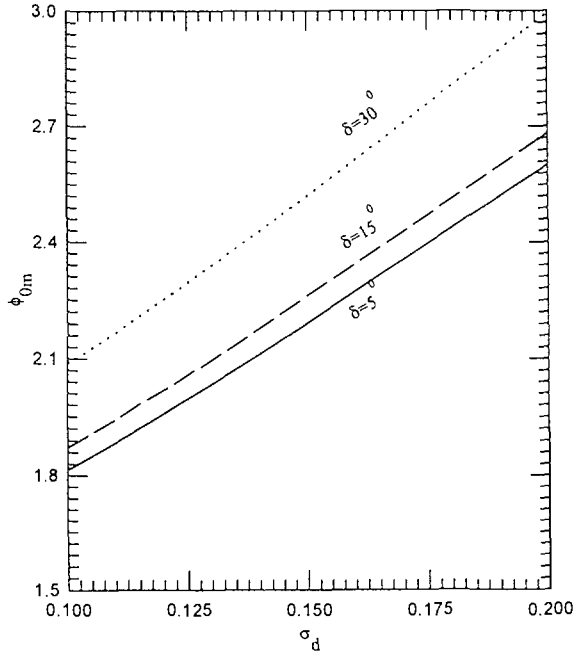
3.0
2.7
2.4
2.1
1.8
1.5
ϕ_{0m}
δ=30°
δ=15°
δ=5°
0.100
0.125
0.150
0.175
0.200
σ_d

Fig.2

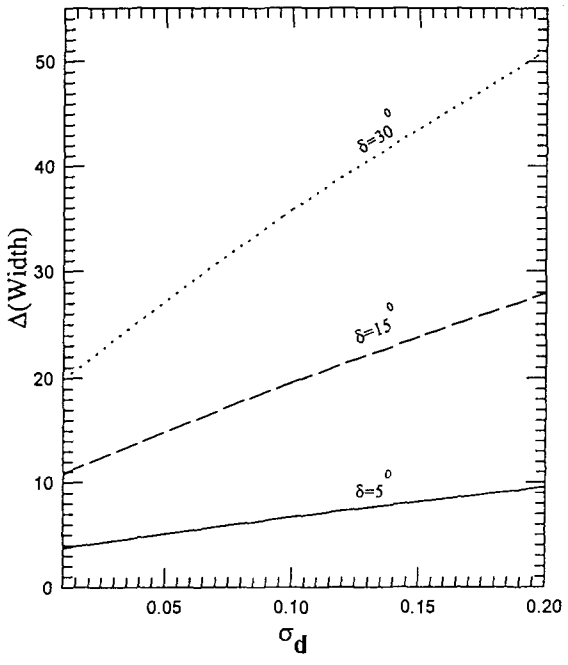
50
40
30
20
10
0
Δ(Width)
δ=30°
δ=15°
δ=5°
0.05
0.10
0.15
0.20
σd

Fig.3

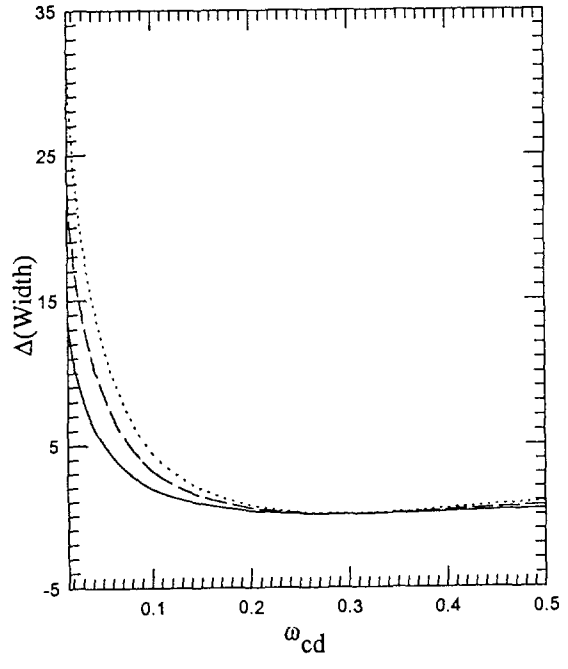
35
25
15
5
-5
Δ(Width)
0.1
0.2
0.3
0.4
0.5
ωcd

Fig.4

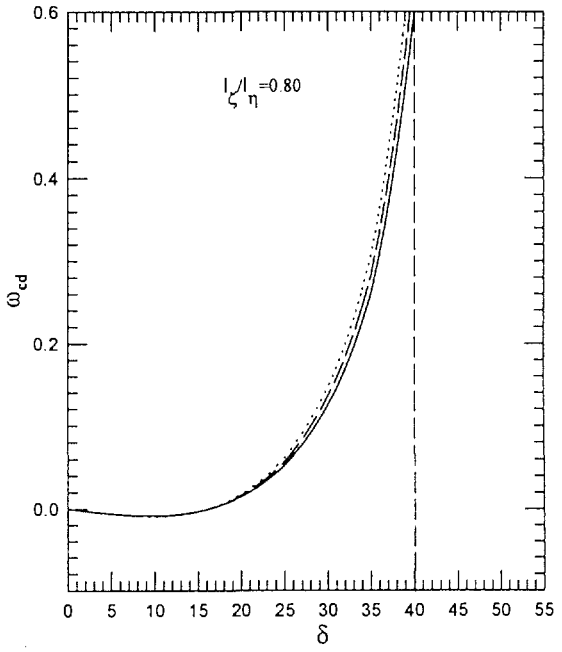
l_ζ/l_η=0.80
ω_{cd}
0.6
0.4
0.2
0.0
0 5 10 15 20 25 30 35 40 45 50 55
δ

Fig.5

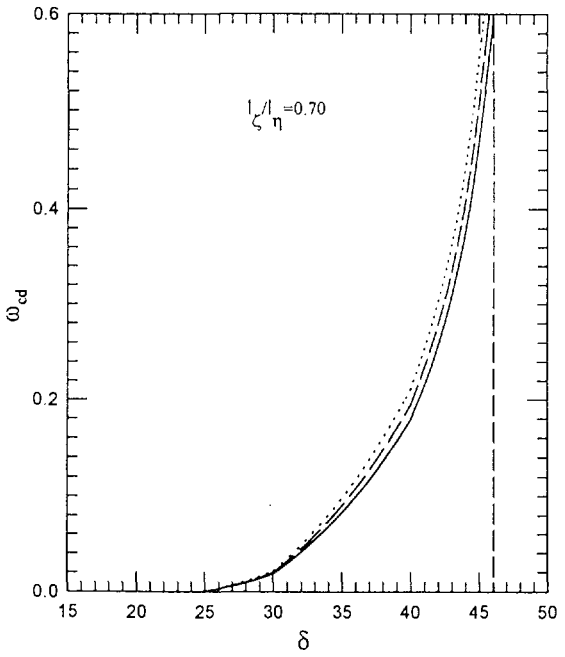
l_ζ/l_η=0.70
ω_{cd}
0.6
0.4
0.2
0.0
15 20 25 30 35 40 45 50
δ

Fig.6

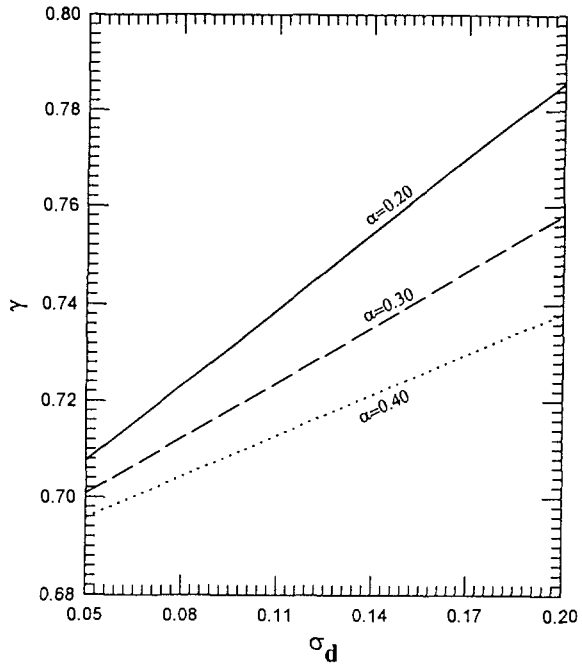
0.80
0.78
0.76
0.74
0.72
0.70
0.68
γ
α=0.20
α=0.30
α=0.40
0.05
0.08
0.11
0.14
0.17
0.20
σd

Fig.7

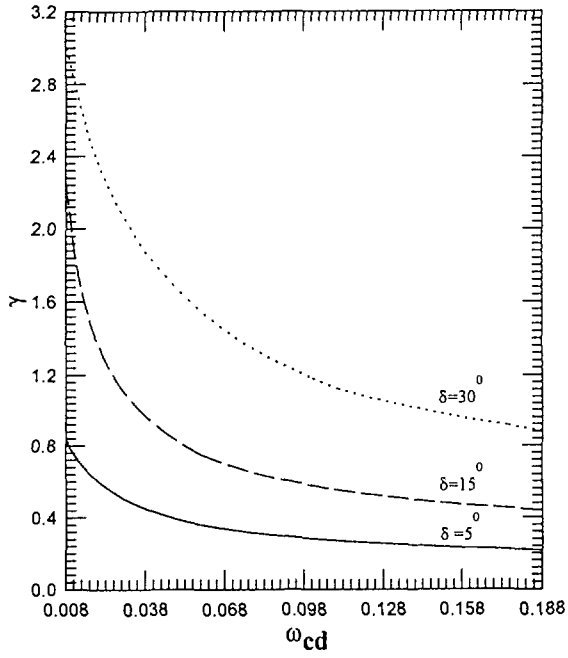
3.2
2.8
2.4
2.0
1.6
1.2
0.8
0.4
0.0
γ
δ=30°
δ=15°
δ=5°
0.008
0.038
0.068
0.098
0.128
0.158
0.188
ωcd

Fig.8